ChemComm

Emergence of intense near-infrared photoluminescence by photoactivation of silver nanoclusters

Journal:	*ChemComm*
Manuscript ID	CC-COM-04-2021-002119.R1
Article Type:	Communication

COMMUNICATION

Emergence of intense near-infrared photoluminescence by photoactivation of silver nanoclusters

Received 00th January 20xx,
Accepted 00th January 20xx

DOI: 10.1039/x0xx00000x

Wataru Ishii,[a] Shohei Katao,[a] Yoshiko Nishikawa,[a] Yasuo Okajima,[a] Atsuya Hatori,[b] Masahiro Ehara,[b] Tsuyoshi Kawai[a] and Takuya Nakashima*[a]

Photoirradiation to a pyridine solution of Ag_{29} nanoclusters (NCs) with red photoluminescence (PL) at 680 nm activated intense PL in the near infrared (NIR) region, giving a PL quantum yield (PLQY) of 33% at 770 nm. The use of Au-doped silver NCs further boosted PLQY more than 45% at 800 nm. The photoirradiation is considered to induce a change in the charge localization in the NCs, leading to the formation of NIR emitting sites.

Development of nanosystems with excellent emission capability has long been a continuing research subject for their importance in the technological applications. While the detailed mechanism of PL origin needs to be further explored, luminescent coinage metal NCs have been attracting much attention.[1-5] They are easier to synthesize compared to molecular and polymer compounds and more biocompatible and less toxic than semiconductor quantum dots (QDs) containing cadmium or lead ions. Silver-based NCs are of particular interest because they often exhibit remarkable PL performance.[6-9] Ag NCs with the composition of $[Ag_{29}(dithiolate)_{12}]^{3-}$ are one of the most studied silver-based luminescent NC groups, whose structures, compositions and optical properties have been extensively characterized including well-defined atomic structures through X-ray crystallography.[10,11] Recent efforts have been devoted to making the $Ag_{29}(dithiolate)_{12}$ NCs more luminescent through strategies employing metal atom doping,[12-15] surface engineering[16-20] and self-assembly.[21-24] Whereas some of those works succeeded in the enhancement of PLQY over 20% for their red PL (λ_{PL} ~ 650 nm),[12,17,24] the development of NCs with strong PL in the NIR region at room temperature still remains an important challenge.[25,26]

In the present study, we demonstrate the stimulation of NIR PL activity in the silver-based NCs with QY over 45% through photoirradiation, which is among the highest values for NIR-emissive NCs so far reported.[26] We achieved such the high QY values in the NIR region with $Ag_{29}(BDT)_{12}(TPP)_4$ NC (BDT: 1,3-benzenedithiol; TPP: triphenylphosphine, Ag_{29} NC) which is one of the representative silver-based NCs. The as-prepared Ag_{29} NCs exhibit an emission band at around 680 nm just after dissolved in pyridine, which shifted to the longer wavelength region over 750 nm by means of visible light irradiation with enhancing the PL intensity. The use of doped-Au_xAg_{29-x} (x = 0~23) NCs for the photoactivation resulted in further red-shift of PL band to 800 nm with larger QYs over 45%. The addition of reductant such as tetrabutylammonium borohydrate ($TBABH_4$) to the light-activated solution restored the PL band at 680 nm with the disappearance of NIR PL activity, suggesting the involvement of photoreacted species.

The Ag_{29} NCs were prepared according to the method reported by Bakr and co-workers.[10] The precipitate formed after the purification process was tested for solubility in various solvents under ambient light condition. In addition to DMF, which was reported as a good solvent,[10] they could be fairly dispersed in pyridine with a red-shifted PL peak (Fig. S1). With careful handling in the dark, the pyridine solution just after the dispersion of NCs was found to give absorption and PL profiles similar to those in a DMF solution (Fig. 1 and Fig. S1), corresponding to the formation of $[Ag_{29}(BDT)_{12}(TPP)_x$ (x = 0–4)]$^{3-}$ compositions. The PL band maximum of Ag_{29} NCs appeared at 680 nm just after the dispersion in pyridine with PLQY of 1% (1.7% in pyridine-d_5, Fig. S2) which is similar to that in DMF (1%).[21] Very interestingly, an emission band at 770 nm appeared with light irradiation at 450 nm in pyridine, which was accompanied by the disappearance of the original one at 680 nm (Fig. 1b). The newly emerging NIR PL band increased with the PLQY up to 33% by the light irradiation for 90 min and the further illumination led to the photodecomposition of NCs. Meanwhile, a gradual decrease was observed in the absorption peaks over 330 nm, indicating the simultaneous

[a] *Division of Materials Science, Graduate School of Science and Technology, Nara Institute of Science and Technology (NAIST), Ikoma, Nara 630-01921, Japan. E-mail: ntaku@ms.naist.jp*
[b] *Institute for Molecular Science, Research Center for Computational Science, Myodaiji, Okazaki 444-8585, Japan.*
†Electronic Supplementary Information (ESI) available: CCDC 2076349. For ESI and crystallographic data in CIF or other electronic format see
DOI: 10.1039/x0xx00000x

photodecomposition of Ag_{29} NCs (Fig. 1a). Excitation spectra monitored at 680 and 770 nm before and after the photoirradiation, respectively, gave a negligible difference (Fig. S3). This result suggests that the fundamental electronic structure of Ag_{29} NCs responsible for light absorption was apparently maintained even after the photoactivation.

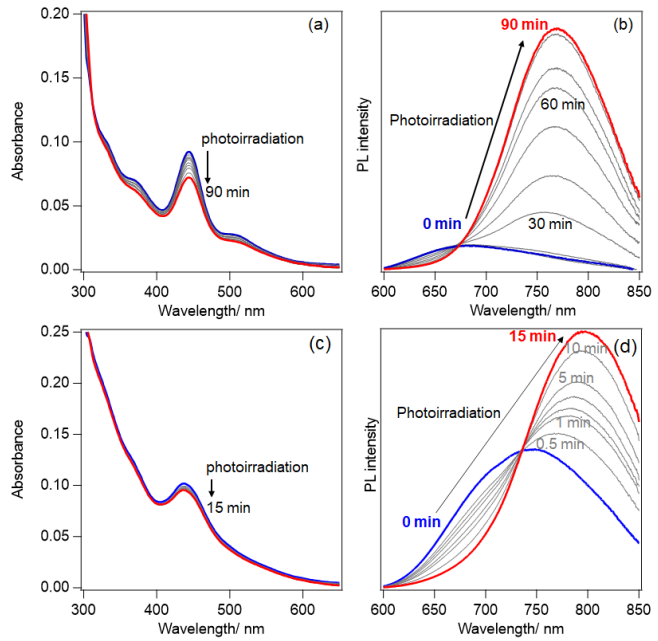

Fig. 1 (a,c) UV-vis and (b,d) PL spectral change of (a,b) Ag_{29} and (c,d) doped Au_xAg_{29-x} NCs in pyridine with light irradiation at 450 nm.

The change in the PL activity was also investigated by emission lifetime study. Since the laser excitation for the PL decay measurement could induce the NIR PL activation simultaneously, the photoactivated sample in pyridine was measured. The PL lifetime of $Ag_{29}(BDT)_{12}(TPP)_x$ (x = 0~4) was reported to vary in the range of 0.07–1.1 μs depending on the concentration of TPP in DMF.[19] The Ag_{29} NCs with the NIR PL activity exhibited a single exponential decay with a time constant (lifetime, τ) of 9.2 μs (Fig. S4), which is 8.5 times longer than that of $Ag_{29}(BDT)_{12}(TPP)_4$ NCs in DMF solution (τ = 1080 ns).[19] This result suggests that the different species or excited state are responsible for the origin of NIR PL.

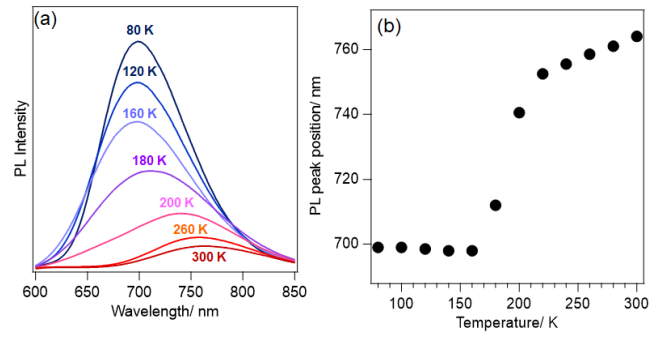

Fig. 2 Temperature-dependent PL study of the photoactivated Ag_{29} NCs in pyridine. (a) PL spectra measured at various temperature (λ_{ex} = 450 nm) and (b) plot of PL peak position as a function of temperature.

Temperature-dependent PL study often provides a useful insight into the excited state properties of emissive NCs.[21] The photoactivated Ag_{29} NCs in pyridine was placed in a cryostat and subjected to temperature-dependent PL study (Fig. 2). Although absolute PL intensity at each temperature is not fairly compared owing to the scattering of frozen medium, it clearly showed a continuous decrease with increasing temperature, suggesting the contribution of phonon-assisted nonradiative decay. The PL peak position was constant at 700 nm in the range of 80–160 K, while it exhibited a sudden red-shift over 180 K and then gradually shifted to 770 nm until 300 K. Such a PL peak shift in response to temperature was absent for the Ag_{29} NCs in DMF.[21] Similar PL-red shift in increasing the temperature has been often observed in the excited state transition from locally excited state (LE) to intramolecular charge transfer (CT) one with an activation barrier in organic fluorescent molecules.[27] Thus the temperature-dependent PL study of photoactivated Ag_{29} NCs suggested an interplay of at least two excited states with different nature in the PL property.

Sigle crystals of the photoactivated Ag_{29} NCs were obtained in a pyridine solution by vapor diffusing diethyl ether. The PL spectrum of a single crystal exhibited an intense emission band around 760 nm (Fig. S5), which is obviously at longer wavelength compared to the crystallized film obtained from a DMF solution (λ_{PL} = 715 nm)[10] and suggests that the crystal is composed of photoactivated Ag_{29} NCs. While the basic structure of $Ag_{29}(BDT)_{12}$ NC was maintained in the crystal, a NC accompanied three sodium cations at specific positions (Fig. 3 and Figs. S6–8, Table S2 for details). The net charge of –3 in a NC should be neutralized by certain cations.[16,23,28] However, there has been no report on the shift of PL peak position to such the NIR region upon specific interactions with counter cations in crystals.[10,16,23,28] Two thiolate moieties in BDT are classified into μ_3- and μ_2-bridging groups coordinating to two and three silver atoms on the NC, respectively, and each sodium cation interacts with the latter one at specific position. That is, the sodium sites are localized on one of four Ag_3S_3 crowns in the shell[10] with binding to three thiolate groups in the identical crown. The interaction led to the slight expansion of Ag_3-triangle (light green) in the crown (Fig. S6). It should be noted that the Na_3-triangle incorporates a nitrate anion (NO_3^-) in the center. These perturbations in the crystal structure described above could be attributed to the generation of NIR emitting site. Meanwhile, three of tetravalent Ag sites (light blue) originally for TPP were bound to pyridine molecules and the remaining site was unoccupied.

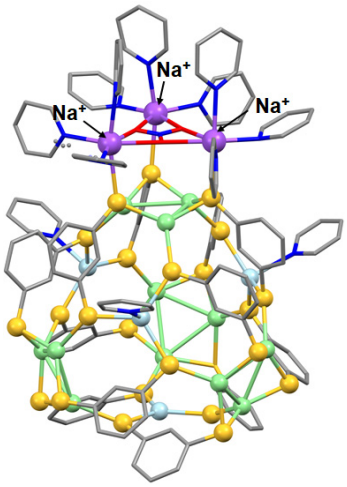

Fig. 3 X-ray crystal structure of photoactivated Ag_{29} NCs obtained in pyridine. H atoms and Ag_{13} centered icosahedral was omitted for clarity. Color labels: Ag, light green and light blue; Na, purple; S, yellow; N, blue; O, red; C, grey.

The photoactivated species were also investigated by electrospray ionization mass (ESI-MS, Figs. S9, S10). The ESI-MS profile contains peaks corresponding to the compositions of $[NaAg_{29}(BDT)_{12}(TPP)_x$ (x = 0~4)$]^{2-}$ in addition to commonly observed peaks for $[Ag_{29}(BDT)_{12}(TPP)_x$ (x = 0~4)$]^{3-}$.[10,23,28] Such peaks corresponding to the compositions with z = –2 were observed for Cs-bound Ag_{29} NCs.[23] Furthermore, each peak accompanies a larger peak with an m/z increase of 42.5 assigned to an $NaNO_3$ adduct ($[Na_2Ag_{29}(BDT)_{12}(TPP)_x(NO_3)$ (x = 0~4)$]^{2-}$ as a sum). We further confirmed a peak, though small, corresponding to the composition of $[Na_3Ag_{29}(BDT)_{12}(NO_3)]^-$ carrying three sodium ions with a nitrate ion (Fig. S10). The result of ESI-MS well accorded with the X-ray crystal structure except that the NC carried TPP instead of pyridine in the MS measurement, suggesting the stronger binding capability of TPP in solution.

In order to obtain an insight into the mechanism for the photoactivation of NIR PL activity, a couple of control experiments were performed. First, an as-dispersed pyridine solution was kept in dark. While another one employed the light irradiation at 450 nm, it was performed for a carefully degassed solution of Ag_{29} NCs. As a result, neither the former nor the latter could induce the NIR PL activity (Fig. S11). Therefore, the light irradiation to the pyridine solution under aerobic condition seems mandatory for the NIR PL activation. Furthermore, the addition of reductant such as $TBABH_4$ or $NaBH_4$ to the pyridine solution with the NIR PL activity reversed the PL peak position with decreasing the PL intensity (Fig. S12). The addition of excess amount of $TBABH_4$ (ca. 10 eq. of Ag_{29} NC) eventually resulted in the complete reproduction of PL peak position at 680 nm without changing the absorption profiles. The PL spectral change with the titration of $TBABH_4$ indicated that the photoactivated Ag_{29} NCs react with the reductant in a stoichiometric manner. The response to the reductant also supports that a chemical change of Ag_{29} NC is responsible for the emergence of bright NIR PL activity, which simultaneously had a negligible effect on the electronic structure in the ground state (light absorption).

The PL decay was also affected by the addition of reductant, changing to a dual exponential profile with time constants of 23 and 160 ns after treating the pyridine solution with excess amount of $TBABH_4$ (ca. 10 eq. of Ag_{29} NC, Fig. S4b). These values were well accorded with those observed for $Ag_{29}(BDT)_{12}(TPP)_x$ NCs with x = 0~1 in DMF, originating from a triplet and/or long-lived CT state.[19] The reduction of Ag_{29} NCs with NIR PL activity most likely restored the original species before the photoactivation. The radiative (k_r) and nonradiative (k_{nr}) constants were estimated from the values of PLQY and lifetime (Table S1). Regardless of the difference in the τ values, both the samples before and after the addition of $TBABH_4$ gave the k_r values with the same order of magnitude (10^4 s^{-1}), suggesting a similar nature of excited state for those PL (triplet and/or long-lived CT state).[17,19] Alternatively, the NIR PL involved the more suppressed nonradiative decay constant (k_{nr} = 7.5×10^4 s^{-1}) compared to the emission at 680 nm (6.1×10^6 s^{-1}).

The PL spectral change induced by mixing DMF to the pyridine solution supported the involvement of pyridine molecule in the formation of NIR PL active sites in solution. The increase of DMF content in the pyridine solution after the photoactivation with keeping the Ag_{29} NC concentration constant resulted in a blue shift together with a continuous decrease in the PL band (Fig. S13). The NIR PL band at 770 nm was almost negligible in a pyridine/DMF (1:9) mixture, wherein much excess amount of pyridine molecules relative to Ag_{29} NCs exist. Given the interaction of pyridine molecule with silver atom is rather dynamic or weak in a chemical equilibrium, the decrease in the pyridine concentration may result in the loss of NIR PL active sites involving Ag-pyridine interaction on the surface of NC.

Here we propose a plausible mechanism on the stimulation of NIR PL activity in the Ag_{29} NCs. The photoirradiation at 450 nm stimulates a charge-transfer excitation from the Ag-thiolate shell to the superatom D-orbitals on the Ag_{13} core.[29,30] The CT state was reported to relax rapidly to a long-lived triplet state (T_1), emitting the red PL in DMF (Fig. 4).[29] This excitation also weakens the Ag-S bonds in the shell, possibly leading to the bond dissociation with the aid of charge transfer to oxygen. The excitation at other absorption bands seemed to also result in the activation of Ag-S bonds (Fig. S14). While the transient dissociation of Ag-S bonds seems to be regenerated rapidly in most media, the strong metal coordinating capability of pyridine enabled the complete bond cleavage. The dissociated Ag atoms were coordinated by the abundant pyridine molecules, forming surface-localized sites responsible for the excited state emitting the bright NIR PL (Fig. 4). There is a thermal energy barrier ($\Delta G^{\ddagger}$) from the original T_1 to the photoactivated state (seemingly a triplet state, T_1') as suggested by the temperature dependent PL study. It should be noted that the dissociated Ag and S might come close in the crystallization (Fig. 3). However, the accumulation of cationic Na^+ ions suggested the localization of negative charge on the sulfur atoms, leading to the detection of Na_3-adducts in the MS measurement. Regardless of species, the cations are considered to stabilize the dissociated thiolates since the use of tetrabutylammonium salt in the preparation of NCs also led to the successful photoactivation of NIR PL (Fig. S15). The addition of reductant ($TBABH_4$) to the photoactivated Ag_{29} NC solution resulted in the regeneration of Ag_{29} NC[20,31] with reconstructing the Ag-S bonds on the surface and diminishing the NIR PL active sites. The reduction treatment also resulted in the marked decrease of peak intensity for Na_2-adducts in the ESI-MS profile (Fig. S9). A preliminary study based on density functional theory (DFT) calculations also suggested the possibility of red-shift in PL by the formation of defect site (Figs. S16, 17, Table S3), whereas a more detailed theoretical investigation is needed to reproduce this photoactivation phenomenon.

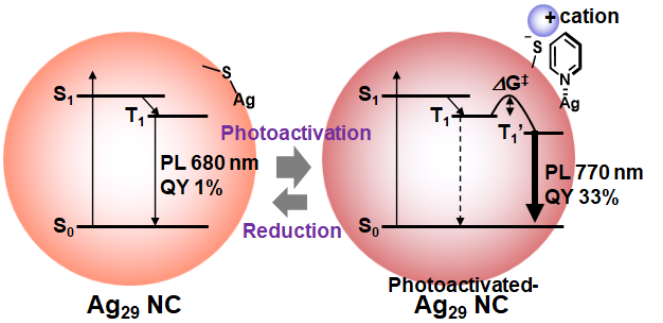

Fig. 4 Jablonski diagram proposing the change of excited state relaxation mechanisms induced by the photoactivation of Ag_{29} NCs. The diagram for Ag_{29} NC before the photoactivation was illustrated on the basis of literature (ref. 29).

Finally, to obtain a further high PLQY value in the NIR region and demonstrate the versality of present mechanism, Au-doped Ag NCs were employed. According to the literature method, 40mol% of gold precursor was mixed in the synthesis of NCs, giving Au-doped NCs with the compositions of $[Au_xAg_{29-x}(BDT)_{12}(TPP)_4$ (x = 0~23)$]^{3-}$ (Fig. S18).[12] The obtained powder was dissolved in pyridine followed by the photoactivation. The original doped Au_xAg_{29-x} NCs exhibited the red emission with the peak position around 700 nm and QY of 25% (Figs. 1c,d, S19). In a similar manner to undoped Ag_{29} NCs, the photoactivation of doped Au_xAg_{29-x} NCs shifted the PL peak to 800 nm and further enhanced the QY more than 45%. This value is higher than those of conventionally used standard NIR emitting organic dyes[32] and almost reaches to those of ultrabright NIR emitting perovskite nanocrystals.[33]

In summary, we have succeeded in the stimulation of ultrabright photoluminescence activity in the NIR-I (700–950 nm) region for the Ag_{29}-based NCs through photoirradiation in pyridine. The formation of Ag-pyridine coordination sites on the surface was suggested as a possible origin of NIR PL activity. As a preliminary result, we found that the similar stimulation of NIR PL could be achieved in the presence of pyridine-tethering polymers. The polymer-NC composites with the NIR-PL activity could be a promising material in theranostics applications,[34] operating as an NIR emitting bioprobe as well as a photosensitizer for superoxides generation.

This work was supported by JSPS KAKEN-HI Grant Numbers JP16H06522 (T.N.) and JP16H06511 (M.E.) in Scientific Research on Innovative Area "Coordination Asymmetry" and by JST CREST Grant Number JPMJCR20B2, Japan.

Conflicts of interest

There are no conflicts to declare.

Notes and references

1 J. P. Wilcoxon and J. E. Martin, *J. Chem. Phys.*, **108**, 9137-9143.
2 X. Kang and M. Zhu, *Chem. Soc. Rev.*, 2019, **48**, 2422-2457.
3 A. Cantelli, G. Guidetti, J. Manzi, V. Caponetti and M. Montalti, *Eur. J. Inorg. Chem.*, 2017, 5068-5084.
4 I. Díez and R. H. A. Ras, *Nanoscale*, 2011, **3**, 1963-1970.
5 M. M. Zhang, K. Li and S. Q. Zang, *Adv. Opt. Mater.*, 2020, **8**, 1902152.
6 C. I. Richards, S. Choi, J. C. Hsiang, Y. Antoku, T. Vosch, A. Bongiorno, Y. L. Tzeng and R. M. Dickson, *J. Am. Chem. Soc.*, 2008, **130**, 5038-5039.
7 H. Xu and K. S. Suslick, *Adv. Mater.*, 2010, **22**, 1078-1082.
8 M. A. Muhammed, F. Aldeek, G. Palui, L. Trapiella-Alfonso and H. Mattoussi, *ACS Nano*, 2012, **6**, 8950-8961.
9 J. Yang and R. Jin, *J. Phys. Chem. C*, 2021, **125**, 2619-2625.
10 L. G. AbdulHalim, M. S. Bootharaju, Q. Tang, S. Del Gobbo, R. G. AbdulHalim, M. Eddaoudi, D. E. Jiang and O. M. Bakr, *J. Am. Chem. Soc.*, 2015, **137**, 11970-11975.
11 M. van der Linden, A. J. van Bunningen, M. U. Delgado-Jaime, B. Detlefs, P. Glatzel, A. Longo and F. M. F. de Groot, *J. Phys. Chem. C*, 2018, **122**, 28351-28361.
12 G. Soldan, M. A. Aljuhani, M. S. Bootharaju, L. G. AbdulHalim, M. R. Parida, A. H. Emwas, O. F. Mohammed and O. M. Bakr, *Angew. Chem. Int. Ed.*, 2016, **55**, 5749-5753.
13 M. S. Bootharaju, S. M. Kozlov, Z. Cao, M. Harb, M. R. Parida, M. N. Hedhili, O. F. Mohammed, O. M. Bakr, L. Cavallo and J. M. Basset, *Nanoscale*, 2017, **9**, 9529-9536.
14 X. Kang, M. Zhou, S. Wang, S. Jin, G. Sun, M. Zhu and R. Jin, *Chem Sci*, 2017, **8**, 2581-2587.
15 M. van der Linden, A. J. van Bunningen, L. Amidani, M. Bransen, H. Elnaggar, P. Glatzel, A. Meijerink and F. M. F. de Groot, *ACS Nano*, 2018, **12**, 12751-12760.
16 M. S. Bootharaju, S. M. Kozlov, Z. Cao, A. Shkurenko, A. M. El-Zohry, O. F. Mohammed, M. Eddaoudi, O. M. Bakr, L. Cavallo and J.-M. Basset, *Chem. Mater.*, 2018, **30**, 2719-2725.
17 E. Khatun, A. Ghosh, P. Chakraborty, P. Singh, M. Bodiuzzaman, P. Ganesan, G. Nataranjan, J. Ghosh, S. K. Pal and T. Pradeep, *Nanoscale*, 2018, **10**, 20033-20042.
18 A. Nag, P. Chakraborty, A. Thacharon, G. Paramasivam, B. Mondal, M. Bodiuzzaman and T. Pradeep, *J. Phys. Chem. C*, 2020, **124**, 22298-22303.
19 Y. Niihori, N. Takahashi and M. Mitsui, *J. Phys. Chem. C*, 2020, **124**, 5880-5886.
20 H. Yoshida, J. Kumar, M. Ehara, Y. Okajima, F. Asanoma, T. Kawai and T. Nakashima, *Bull. Chem. Soc. Jpn.*, 2020, **93**, 834-840.
21 X. Kang, S. Wang and M. Zhu, *Chem Sci*, 2018, **9**, 3062-3068.
22 M. A. H. Muhammed, L. K. Cruz, A. H. Emwas, A. M. El-Zohry, B. Moosa, O. F. Mohammed and N. M. Khashab, *Angew. Chem. Int. Ed.*, 2019, **58**, 15665-15670.
23 X. Wei, X. Kang, Q. Yuan, C. Qin, S. Jin, S. Wang and M. Zhu, *Chem. Mater.*, 2019, **31**, 4945-4952.
24 X. Kang, X. Wei, S. Jin, S. Wang and M. Zhu, *Inorg. Chem.*, 2021, **60**, 4198-4206.
25 S. E. Crawford, M. J. Hartmann and J. E. Millstone, *Acc. Chem. Res.*, 2019, **52**, 695-703.
26 A. S. Krishna Kumar and W.-L. Tseng, *Anal. Methods*, 2020, **12**, 1809-1826.
27 T. Inouchi, T. Nakashima, M. Toba and T. Kawai, *Chem. Asian J.*, 2011, **6**, 3020-3027.
28 X. Kang, X. Wei, P. Xiang, X. Tian, Z. Zuo, F. Song, S. Wang and M. Zhu, *Chem. Sci.*, 2020, **11**, 4808-4816.
29 A. P. Veenstra, L. Monzel, A. Baksi, J. Czekner, S. Lebedkin, E. K. Schneider, T. Pradeep, A. N. Unterreiner and M. M. Kappes, *J. Phys. Chem. Lett.*, 2020, **11**, 2675-2681.
30 H. Yoshida, M. Ehara, U. D. Priyakumar, T. Kawai and T. Nakashima, *Chem. Sci.*, 2020, **11**, 2394-2400.
31 M. van der Linden, A. Barendregt, A. J. van Bunningen, P. T. Chin, D. Thies-Weesie, F. M. de Groot and A. Meijerink, *Nanoscale*, 2016, **8**, 19901-19909.
32 K. Rurack and M. Spieles, *Anal. Chem.*, 2011, **83**, 1232-1242.
33 R. Begum, X. Y. Chin, M. Li, B. Damodaran, T. C. Sum, S. Mhaisalkar and N. Mathews, *Chem. Commun.*, 2019, **55**, 5451-5454.
34 Y. Yang, Y. Zhou, S. Wang, X. Wang, X. Liu, A. Xie, Y. Shen and M. Zhu, *Chem. Commun.*, 2020, **56**, 9842-9845.